Journal of Statistical Physics, Vol. 39, Nos. 5/6, 1985

Propagation of Solitary Waves in Channels of Decreasing Depth

C. J. Knickerbocker[1] and Alan C. Newell[2]

The changes which occur in a right-going solitary wave as it travels a channel of decreasing depth are discussed. In addition to the changes in the solitary wave, we have found through a judicious use of the conservation laws two secondary structures (a shelf and a reflection). Each of these structures is small with respect to the solitary wave, though the mass flux associated with each is of the same order as that of the solitary wave. Of interest is that the amplitude of the reflected wave does not satisfy Green's law. But rather, the amplitude of the reflected wave is constant along left-going characteristics. This finding allows us to satisfy the mass flux conservation laws to leading order and establishes the perturbed Korteweg–deVries equation as a consistent approximation for the right-going profile.

KEY WORDS: Korteweg-deVries; solitary wave; Green's law; variable depth.

1. INTRODUCTION

For over 100 years many investigators have been interested in models which represent the changes that occur in a solitary wave as it travels over a slowly changing topography. We shall consider a mathematical model based upon the following assumptions regarding the physical situation. First, the solitary wave is considered long with respect to the depth, that is to say the ratio l/D is large (Fig. 1). Second, we shall consider only low-amplitude solitary waves or that the ratio a/D is small. Third, we are assuming that the depth of the water is slowly varying or l/L is small or that the order-one changes in the depth occur over many solitary wave widths.

[1] St Lawrence University, Department of Mathematics, Canton, New York 13617.
[2] Program in Applied Mathematics, University of Arizona, Tucson, Arizona 85721.

0022-4715/85/0600-0653$04.50/0

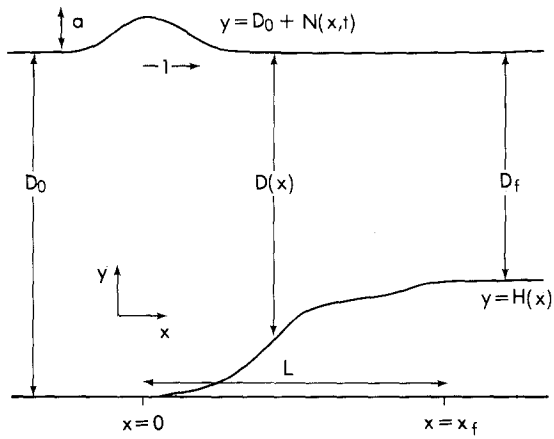

Fig. 1. Physical system being considered, where $N(x, t)$ is the dimensional elevation, $U(x, t)$ is the dimensional horizontal velocity, x is space coordinate, t is time, and $D(x)$ is the depth. For $x<0$, $D(x)=D_0$ and for $x>x_f$, $D(x)=D_f$.

Under these assumptions, what are the effects of a slowly decreasing channel depth on a long low-amplitude solitary wave?

1. The solitary wave will slowly distort.
2. A secondary structure (a shelf) will be created and will travel in the lee of the solitary wave.
3. Another structure will be created in the form of a reflection which travels away from the solitary wave and shelf.

We can establish the leading order components of the flow (where by leading order we mean any component of the flow which contains an order-one amount of mass) through a judicious use of particular conservation laws of the model. The steps of the analysis are as follows:

First, since the depth is varying (Fig. 1), some of the water will be reflected as the solitary wave travels from $x=0$ to $x=x_f$. In other words, the amount of water passing $x=x_f$ is less than the amount of water passing $x=0$. The rule for this shore bound (this will also be called unidirectional or right-going from the orientation of the figures) mass flux is

$$\frac{\delta}{\delta x}\int_{-\infty}^{\infty} \rho D(x)\, U(x, t)\, dt = 0 \tag{1.1}$$

[where x is space, t is time, $D(x)$ is the local depth, $U(x, t)$ the horizontal velocity, ρ the density, g the gravity, D_0 the constant local depth for $x<0$], which shall be referred to as the conservation of unidirectional mass flux.

The water which was reflected, as the solitary wave traveled from $x=0$

to $x = x_f$, will pass $x = 0$. Therefore, the total amount of mass flux at $x = 0$ (unidirectional mass flux at $x = 0$ plus the reflected mass flux) is equal to the total mass flux at $x = x_f$. This is written as

$$\rho D_0^{1/4} \frac{\delta}{\delta x} \int_{-\infty}^{\infty} D^{3/4}(x)\, U(x, t)\, dt = 0 \tag{1.2}$$

which shall be referred to as the total conservation of mass flux law.

Second, as the variation in the depth is felt by the solitary wave

$$N(x, t) = \frac{4}{3} \eta_0^2 D_0 \varepsilon \operatorname{sech}^2 \eta_0 \left[-\frac{t(\varepsilon g)^{1/2}}{(D_0)^{1/2}} + \frac{\varepsilon^{1/2} x}{D_0} - \frac{2\eta_0^2 \varepsilon^{3/2} x}{3D_0} \right], \qquad x < 0 \tag{1.3}$$

[where $N(x, t) = D^{1/2} U(x, t)/g^{1/2}$ is the surface elevation] it will begin to distort. These distortions in the amplitude, shape, and speed can be calculated using the center of gravity and conservation of energy law, yielding

$$U_s(x, t) = \tfrac{4}{3} \eta_0^2 D_0^2 \varepsilon g^{1/2} D^{-3/2} \operatorname{sech}^2(\eta_0 R) + O(\varepsilon\sigma)$$

where

$$R = -\frac{t(\varepsilon g)^{1/2}}{D_0} + \frac{\varepsilon^{1/2} x}{D_0} - \frac{2\eta_0^2 \varepsilon^{3/2} x}{3D_0} \tag{1.4}$$

The mass flux associated with the solitary wave, $\frac{8}{3} \eta_0 \rho \varepsilon^{1/2} D_0 D$, does not fulfill the mass flux requirement for either the total flow (1.2) or unidirectional flow (1.1). The small parameter $D_0 \varepsilon^{1/2}$ is found from the amplitude of the incoming solitary wave (1.3). What happens is that the solitary wave reacts to the changing depth by dropping off small amounts of water. Some of the water will travel behind the solitary wave forming a right-going shelf and some of the water will travel away from the solitary wave forming a left-going wave of reflection.

Third, the water dropped along the path of the solitary wave, forming the shelf, can be found from the difference between the rate of change of the unidirectional mass flux and the of rate of change of the mass flux of the solitary wave. The right-going shelf is small with respect to the solitary wave and can therefore be treated as a linear model, and its evolution along right-going characteristics is given by Green's law (the amplitude is inversely proportional to the fourth root of the depth). The horizontal velocity of the shelf is given by

$$U_+(x, t) = \frac{-3}{\eta_0 (D_0 \varepsilon)^{1/2}} \frac{dD}{dx} D^{-3/4}(x)\, D^{9/4}(\bar{x}) + O(\varepsilon\sigma^2) \tag{1.5}$$

where $\bar{x}$ is the current position of the solitary wave. The shelf is finite in extent and exists between the right-going linear characteristic which passes through the point where the depth begins to change

$$\hat{\Theta}_+ = -t(g\varepsilon)^{1/2}/(D_0)^{1/2} + \int_0^{x\varepsilon^{1/2}/D_0} [D_0/D(r)]^{1/2}\, dr = 0 \tag{1.6}$$

and the solitary wave. Even though the shelf is small in amplitude, over distances in which the depth changes by an order-one amount, the shelf is long and the mass flux associated with it is

$$\tfrac{8}{3}\eta_0 \rho \varepsilon^{1/2} D_0^{7/4} D^{1/4} - \tfrac{8}{3}\eta_0 \rho \varepsilon^{1/2} D_0 D$$

which is of the same order as the mass flux of the solitary wave.

Fourth, the reflected wave can be calculated in a manner similar to that used to calculate the shelf. By comparing the rate of change of the total mass flux and the right-going mass flux (the mass flux consisting of solitary wave and shelf), we can calculate the reflection at the lee of the right-going flow. Its evolution, along left-going characteristics, is given by a new law[11]: the amplitude of the reflection is constant along left-going characteristics. The horizontal velocity of the reflected wave is given by

$$U_-(x, t) = \frac{\eta_0 \varepsilon^{1/2} D_0^{9/4}}{3} D_x D^{-1/2}(\bar{x})\, D^{-1}(x) + O(\varepsilon^2 \sigma^2) \tag{1.7}$$

Over distances by which the depth changes by an order-one amount, the length of the reflection is very long, stretching from $\Theta_+ = 0$, to

$$\hat{\Theta}_- = t(g\varepsilon)^{1/2}/(D_0)^{1/2} + \int_0^{x\varepsilon^{1/2}/D_0} [D_0/D(r)]^{1/2}\, dr = 0 \tag{1.8}$$

so that the mass flux associated with the reflection is of the same order as the mass flux of the solitary wave or the right-going shelf. That is

$$\tfrac{8}{3}\eta_0 \rho \varepsilon^{1/2} D_0^{7/4} D_f^{1/4} - \tfrac{8}{3}\eta_0 \rho \varepsilon^{1/2} D_0^{7/4} D^{1/4}$$

The total mass flux, which is found by adding the mass flux due to each portion of the solution, is $\tfrac{8}{3}\eta_0 \rho \varepsilon^{1/2} D_0^{7/4} D_f^{1/4}$ and is equal to the flux of all right-going disturbances at the point after which no further depth changes occurs. These results are established in Section 2 and are confirmed with numerical experiments in Section 3.

History

The mathematical analysis of the surface wave model has been ongoing for the last 150 years.

One of the first studies was conducted by Green in 1832. He studied the effects of a slowly changing depth on a linear surface wave and found that the amplitude of the linear wave changed inversely proportional to the fourth root of the depth. This was to become known as Green's law. Forty years later, Boussinesq[1] was able to show, by invoking the conservation of energy requirement, that the amplitude of a solitary wave changed inversely proportional to the depth. He also noticed that the total conservation of mass flux requirement could not be satisfied by the changing solitary wave. Then in 1895, Korteweg and deVries[12] introduced their model for unidirectional flow over a constant depth and also found solitary wave solutions.

In the early nineteen seventies Kakutani[6] and Johnson[4,5] independently derived a variation of the Korteweg–deVries equation (PKdV) which governs unidirectional flow of weakly nonlinear waves over a slowly changing depth. A number of articles appeared in the literature within the next few years attempting to solve PKdV both analytically and numerically. These included attempts by Grimshaw,[2,3] who by invoking the conservation of energy requirement showed that the amplitude of the solitary wave changed inversely proportional to the depth. He also observed that "the mass contained in the wave is not conserved." The solution of this model was the subject of several articles by Johnson[4,5] in which he attempted to solve the model both analytically and numerically. His earlier articles were concerned with the production of new solitary wave as the solitary wave traveled onto a shoal of constant depth. Leibovich and Randall[13] discovered the existence of the shelf numerically but could not find a uniform perturbation solution. They did obtain a nonuniform solution which became a constant rather than decaying as x became large and negative (a result also found by Johnson) and therefore contained an infinite amount of mass.

The difficulty with the infinite mass was corrected by Kaup and Newell.[8] By using the inverse scattering transform they monitored the effects of the perturbation on the scattering data. They found that the shelf was of finite extent and showed that the rate of change in the solitary wave mass was balanced by the rate of change in the mass of the shelf. In 1980 Knickerbocker and Newell[9] extended these results by describing the evolution of the shelf and verifying the results numerically.

Much earlier, Peregrine[16] attempted to solve the full two-directional model. He was successful in approximating the initial amplitude of the

reflected wave with the use of characteristics (he did not mention the existence of the shelf). He also made qualitative comparisons with a numerical simulation. In 1979, Miles[14] also calculated the initial amplitude of the reflection, but he then used Green's law to describe the subsequent evolution of the reflected wave. In 1984, Knickerbocker and Newell[11] discovered a new law for governing the evolution of the reflection.

Recently, some controversy has arisen regarding whether the reflected wave actually exists. Numerical simulations of the full two-directional wave gives convincing evidence of the size, shape, and existence of the reflection.

2. ANALYSIS

The shallow water equations which describe the total flow (the propagation of a solitary wave and its trailing and reflected shelves) are, in nondimensional coordinates,

$$n_t + (hu)_x = -\varepsilon(un)_x + \frac{\varepsilon}{6} h^3 u_{xxx} \tag{2.1}$$

$$u_t + n_x = -\varepsilon u u_x + \frac{\varepsilon}{2} h^2 u_{xxt} \tag{2.2}$$

The equations are the kinematic boundary condition for the free surface and the horizontal momentum equation, respectively. In Eqs. (2.1), (2.2), $n(x, t)$ $(=N/D_0)$, $u(x, t)$ $[=U/(\varepsilon(gD_0)^{1/2})]$, x $(=x\varepsilon^{1/2}/D_0)$ and t $[=t(g\varepsilon)^{1/2}/(D_0)^{1/2}]$ are the nondimensional elevation, horizontal velocity to leading order ($\bar{u} = u + \varepsilon h^2 u_{xx}/2$, where $\bar{u}$ is the horizontal velocity at the surface), horizontal distance, and time variables, respectively. The nondimensional depth $h(x) = D(x)/D_0$ changes from unity to D_f/D_0 in a distance $x_f = O(1/(\varepsilon^{3/2}\sigma))$, where $0 < \varepsilon \ll \sigma \ll 1$, which is long with respect to the width of the solitary wave and the length of the right-going shelf. The small parameter σ is determined from the equation

$$D\left(\frac{D_0}{\varepsilon^{1/2}} \frac{1}{\varepsilon\sigma} x_f\right) = D_f$$

once x_f and D_f are given. Note that in dimensionless coordinates, the amplitude of the solitary wave is order one, its width is order one; the amplitude of the right-going trailing shelf is order σ, its length is order $1/\sigma$ (Fig. 2); the amplitude of the reflected wave is order $\varepsilon\sigma$ and its length is order $1/\varepsilon\sigma$ (Fig. 3). To leading order in ε, the conservation law for the mass

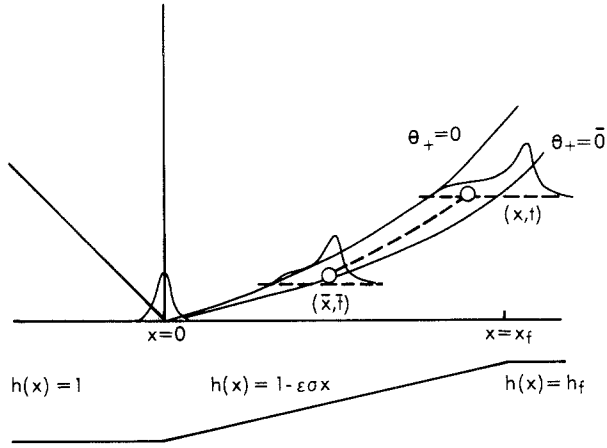

Fig. 2. This figure shows the evolution of a portion of the right-going shelf. The point $(\bar{x}, \bar{t})$ is the point of creation and the dashed line (– – –) corresponds to the positive characteristic passing through $(\bar{x}, \bar{t})$ and (x, t).

flux (the amount of water crossing a fixed station for all time) is, from (2.1),

$$\frac{\partial}{\partial x}\int_{-\infty}^{\infty} h(x)\, u(x, t)\, dt = 0 \tag{2.3}$$

We may look for solutions n_+ and u_+ of (2.1) and (2.2) which depend on the right-going characteristic

$$\Theta_+ = -t + \int_0^x \frac{dr}{[h(r)]^{1/2}}$$

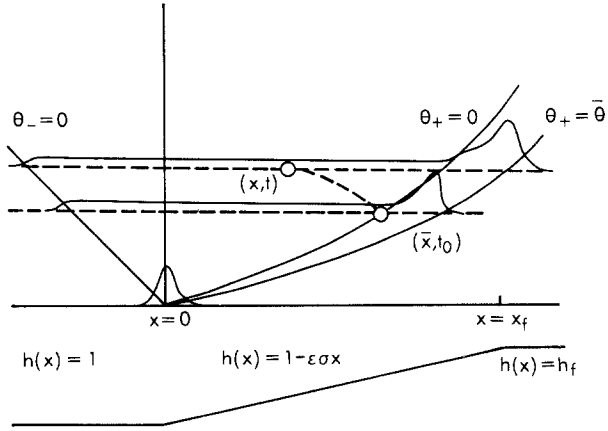

Fig. 3. This figure shows the evolution of a portion of the left-going reflection. The point $(\bar{x}, t_0)$ is the point in space-time where the reflection measured at (x, t) is created. The negative characteristic $\Theta_- = t + \int_0^x h^{-1/2}(r)\, dr$. The dashed line corresponds to the negative characteristic passing through $(\bar{x}, t_0)$ and (x, t).

and slowly on X ($X=\varepsilon x$). In this situation, one finds that, to leading order,

$$n_+ = h^{1/2}u_+ \tag{2.4}$$

$$\left(\frac{\partial}{\partial t}+h^{1/2}\frac{\partial}{\partial x}\right)(h^{3/4}u_+)=\varepsilon\left(-\frac{3}{2}h^{3/4}u_+\frac{\partial u_+}{\partial x}-\frac{1}{6}h^{13/4}\frac{\partial^3 u_+}{\partial x^3}\right) \tag{2.5}$$

and

$$\left(\frac{\partial}{\partial t}+h^{1/2}\frac{\partial}{\partial x}\right)(h^{1/4}n_+)=\varepsilon\left(-\frac{3}{2}h^{-1/4}n_+\frac{\partial n_+}{\partial x}-\frac{1}{6}h^{11/4}\frac{\partial^3 n_+}{\partial x^3}\right) \tag{2.6}$$

Note that the linear portions of (2.5) and (2.6) are Green's law; $h^{3/4}u_+$ and $h^{1/4}n_+$ are constants along the right-going characteristics

$$\Theta_+ = -t+\int_0^x \frac{dr}{[h(r)]^{1/2}}$$

In terms of Θ_+ and X, the transformation of $n_+(x, t)$ to $n(\Theta_+, X)$ yields the perturbed Korteweg–deVries equation,

$$n_X+\frac{3}{2}h^{-3/2}nn_{\Theta_+}+\frac{1}{6}h^{1/2}n_{\Theta_+\Theta_+\Theta_+}=-\frac{1}{4}\left(\frac{h_X}{h}\right)n \tag{2.7}$$

and similarly for $u(\Theta_+, X)$,

$$u_X+\frac{3}{2}h^{-1}uu_{\Theta_+}+\frac{1}{6}h^{1/2}u_{\Theta_+\Theta_+\Theta_+}=-\frac{3}{4}\left(\frac{h_X}{h}\right)u \tag{2.8}$$

From (2.8) we find that

$$\frac{\partial}{\partial X}\int_{-\infty}^{\infty} h^{3/4}(X)\,u_+(\Theta_+, X)\,d\Theta_+ = 0 \tag{2.9}$$

In order to solve (2.5) under the initial boundary conditions

$$n_+(0, t)=u_+(0, t)=\tfrac{4}{3}\eta_0^2\,\mathrm{sech}^2(\eta_0 t), \qquad t\geqslant 0$$
$$n_+(x, 0)/\sqrt{h}=u_+(x, 0)=0, \qquad x\geqslant 0$$

we assume a solution of the form

$$\begin{aligned} n_+(x, t) &= n_s(x, t)+\bar{n}_+(x, t)\\ u_+(x, t) &= u_s(x, t)+\bar{u}_+(x, t)\end{aligned} \tag{2.10}$$

where $n_s(x, t)$ and $u_s(x, t)$ are the amplitude and velocity of the solitary wave, respectively, and $\bar{n}_+(x, t)$ and $\bar{u}_+(x, t)$ denote the amplitude and velocity of the right-going shelf, respectively [note the shelf is order σ in magnitude and nonzero only between $\Theta_+ = 0$ and $\Theta_+ = \bar{\Theta}$, the position of the solitary wave (Fig. 2)].

To find the changes in the solitary wave $[n_s(x, t), u_s(x, t)]$, we assume a leading order solution of the form

$$u_s(x, t) = u_s(\Theta_+, X) = A(X)\,\mathrm{sech}^2[w(X)(\Theta_+ - \bar{\Theta})]$$

From (2.8) we find that

$$A(x) = \tfrac{4}{3}h^{3/2}w^2(X)$$

and (2.11a)

$$\bar{\Theta}_X = \tfrac{2}{3}\eta_0^2 h^{-5/2}(X)$$

From the conservation of energy

$$\frac{\partial}{\partial X}\int_{-\infty}^{\infty} h^{3/2}(X)\,u^2(\Theta_+, X)\,d\Theta_+ = 0$$

we find that

$$\frac{\partial}{\partial X}\left(\frac{h^{3/2}A^2}{w}\right) = 0 \tag{2.11b}$$

By combining (2.11a) and (2.11b) we find that $A(X) = \frac{4}{3}\eta_0^2 h^{-3/2}(x)$ and $w(X) = \eta_0 h^{-3/2}(X)$.

Therefore,

$$u_s(x, t) = \tfrac{4}{3}\eta_0^2 h^{-3/2}\,\mathrm{sech}^2[\eta_0 h^{-3/2}(\Theta_+ - \bar{\Theta})] \tag{2.12a}$$

and from (2.4), the amplitude of the solitary wave is

$$n_s(x, t) = \tfrac{4}{3}\eta_0^2 h^{-1}\,\mathrm{sech}^2[\eta_0 h^{-3/2}(\Theta_+ - \bar{\Theta})]$$

The mass flux associated with this component is

$$m_s(x) = \tfrac{8}{3}\eta_0 h(x) \tag{2.12b}$$

Using (2.4) and approximating the x derivatives on the right-hand side of (2.5) with t derivatives, we find that

$$\frac{\partial}{\partial x}\int_{-\infty}^{\infty} h^{3/4}(x)\,u_+(x, t)\,dt = 0 \tag{2.13}$$

Therefore, under the assumptions made in (2.10), we have

$$\frac{\partial}{\partial x}\int_{\bar{t}(x)}^{t_0(x)} h^{3/4}\bar{u}_+\,dt = -\frac{\partial}{\partial x}\int_{-\infty}^{\infty} h^{3/4}u_s\,dt \tag{2.14}$$

where $t=\bar{t}(x)$ and $t=t_0(x)$ correspond to $\Theta_+=\bar{\Theta}$ and $\Theta_+=0$, respectively (Fig. 2). Since $\bar{u}_+(x,t)$ is assumed small and therefore changes according to the linear portion of (2.5), we have, upon differentiating the left-hand side of (2.14),

$$\bar{u}_+(\bar{x},\bar{t}) = \frac{-3h_x(\bar{x})\,h^{3/2}(\bar{x})}{\varepsilon\eta_0}$$

where we have used the fact that $h^{3/4}\bar{u}_+$ is constant and where $(\bar{x},\bar{t})$ belongs to the path of the solitary wave (Fig. 2). From Green's law, which is valid because the change in $\bar{u}_+$ is fast with respect to the change in $h(x)$,

$$\bar{u}_+(x,t) = \frac{-3}{\varepsilon\eta_0}h^{-3/4}(x)\,h^{9/4}(\bar{x})\,h_x(\bar{x}) \tag{2.15}$$

for any (x,t) lying between the solitary wave path $\Theta_+=\bar{\Theta}$ and $\Theta_+=0$, and $(\bar{x},\bar{t})$ is the point at which the right-going characteristic through (x,t) meets $\Theta_+=\bar{\Theta}$ (Fig. 2). The amplitude of the shelf can be found from (2.4), yielding

$$\bar{n}_+(x,t) = \frac{-3}{\varepsilon\eta_0}h^{-1/4}(x)\,h^{9/4}(x)\,h_x(\bar{x})$$

A little calculation[9] shows that the mass flux $\bar{m}_+$ associated with the shelf component of the flow is

$$\bar{m}_+(x) = \int_{-\infty}^{\infty} h(x)\,\bar{u}_+(x,t)\,dt = \frac{8}{3}\eta_0 h^{1/4}(x) - \frac{8}{3}\eta_0 h(x) \tag{2.16}$$

which, when added to the mass flux (2.12b) associated with the solitary wave gives $\frac{8}{3}\eta_0 h^{1/4}(x)$, which satisfies the equation for the right-going flux, but not (2.3), the total mass flux requirement.

In order to compensate for this discrepancy, it is necessary to add a left-going component $n_-(x,t)$ and $u_-(x,t)$ to the solution. Because of their very small amplitudes, $n_-(x,t)$ and $u_-(x,t)$ will satisfy the linearized versions of equations (2.1) and (2.2). The reflection will be nonzero in the region bounded by $\Theta_-=0$ and $\Theta_+=0$ (Fig. 3). We first calculate their

values along $\Theta_+ = 0$ using the local conservation of mass flux. From (2.3) we have

$$\frac{\partial}{\partial x}\int_{-\infty}^{\infty} [h(x)\, u_+(x, t) + h(x)\, u_-(x, t)]\, dt = 0$$

Therefore,

$$\begin{aligned}\frac{\partial}{\partial x}\int_{-\infty}^{\infty} h(x)\, u_-(x, t)\, dt &= -\frac{\partial}{\partial x}\int_{-\infty}^{\infty} h(x)\, u_+(x, t)\, dt \\ &= -\frac{\partial}{\partial x} h^{1/4}(x)\int_{-\infty}^{\infty} h^{3/4}(x)\, u_+(x, t)\, dt \\ &= -\tfrac{2}{3}\eta_0 h^{-3/4}(x)\, h_x(x), \qquad x < \bar{x}\end{aligned}$$

When the solitary wave is at $(\bar{x}, t_0)$ (Fig. 3), the reflection contributed by the solitary wave up to that point will be nonzero from $t = t_0(x)$, which is the right-going characteristic $\theta_+ = 0$, and $t = t_-(x)$, which is the left-going characteristic initiated at $(\bar{x}, t_0)$. Therefore,

$$\frac{\partial}{\partial x}\int_{-\infty}^{\infty} h(x)\, u_-(x, t)\, dt = \frac{\partial}{\partial x}\int_{t_0(x)}^{t_-(x)} h(x)\, u_-(x, t)\, dt$$

and

$$\frac{\partial}{\partial x}\int_{t_0(x)}^{t_-(x)} h(x)\, u_-(x, t)\, dt = -\frac{2}{3}\eta_0 h^{-3/4}(x)\, h_x(x), \qquad x < \bar{x} \tag{2.17}$$

We differentiate the integral in (2.17), add and subtract $h(x)\, u_-(x, t_0)$, and use $[h(x)\, u_-(x, t)]_x = -n_{-t}$ to find that

$$\begin{aligned}h(x)\, u_-(x, t_0) = {} & \tfrac{1}{3}\eta_0 h^{-1/4}(x)\, h_x(x) \\ & - \tfrac{1}{2}\sqrt{h}\,[n_-(x, t_-) + \sqrt{h}\, u_-(x, t_-)] \\ & + \tfrac{1}{2}\sqrt{h}\,[n_-(x, t_0) + \sqrt{h}\, u_-(x, t_0)]\end{aligned} \tag{2.18}$$

In particular (2.18) holds as x tends to $\bar{x}$, whence t_- tends to t_0. This is how Miles[14] calculated $u_-(\bar{x}, t_0)$. However Eq. (2.18) yields two pieces of information. First,

$$u_-(\bar{x}, t_0) = \tfrac{1}{3}\eta_0 h^{-5/4}(\bar{x})\, h_x(\bar{x}) \tag{2.19}$$

Second, we obtain that

$$(n_- + \sqrt{h}\, u_-)\,|_{t_-} = (n_- + \sqrt{h}\, u_-)\,|_{t_0} \tag{2.20}$$

for any t_- and therefore $n_- + \sqrt{h}\, u_-$ is independent of time at any fixed x, that is,

$$\frac{\partial}{\partial t}(n_- + \sqrt{h}\, u_-) = 0 \tag{2.21}$$

In order to calculate $u_-(x, t)$ for points (x, t) (Fig. 3) in the region bounded by $\Theta_- = 0$ and $\Theta_+ = 0$, Miles applied Green's law to (2.19); that is, he took $h^{3/4}u_-$ constant along left-going characteristics. He also took $h^{1/4}n_-$ equal to $-h^{3/4}u_-$ to leading order. However, this leads to the total mass flux being $\frac{2}{3}\eta_0 h^{1/4} \ln(h_f/h) - \frac{8}{3}\eta_0 h^{1/4}$, which is clearly not constant. What is wrong?

It is incorrect to assume that Green's law holds for left-going disturbances. Green's law only holds when the depth $h(x)$ changes slowly with respect to the gradient of the disturbances in question. On the other hand, the reflected wave, by the very manner in which it is created, has a horizontal gradient which is of the same order as the gradient of the depth. However, Eq. (2.21)

$$n_{-t} + \sqrt{h}\, u_{-t} = 0$$

together with $n_{-t} + (hu_-)_x = 0$ gives us that

$$\left(\frac{\partial}{\partial t} - h^{1/2}\frac{\partial}{\partial x}\right)(hu_-) = 0 \tag{2.22a}$$

and

$$\left(\frac{\partial}{\partial t} - h^{1/2}\frac{\partial}{\partial x}\right)(n_-) = 0 \tag{2.22b}$$

which means that hu_- (and also n_-) is constant along left-going characteristics. Thus for a point (x, t) in the region bounded by $\Theta_- = 0$ and $\Theta_+ = 0$ the velocity of the reflected wave is

$$u_-(x, t) = \tfrac{1}{3}\eta_0 h_x(\bar{x})\, h^{-1/4}(\bar{x})\, h^{-1}(x) \tag{2.23}$$

The reflected mass flux measured along a constant x ($x = x_c$, Fig. 4), can be found by integrating the following expression:

$$\int_{-\infty}^{\infty} h(x_c)\, u_-(x_c, t)\, dt \tag{2.24}$$

But, as the right-going flow travels from $x = x_c$ to $x = x_p$, the reflected mass flux will be nonzero only between $(x_c, t_0(x_c))$ (which lies on the right-going

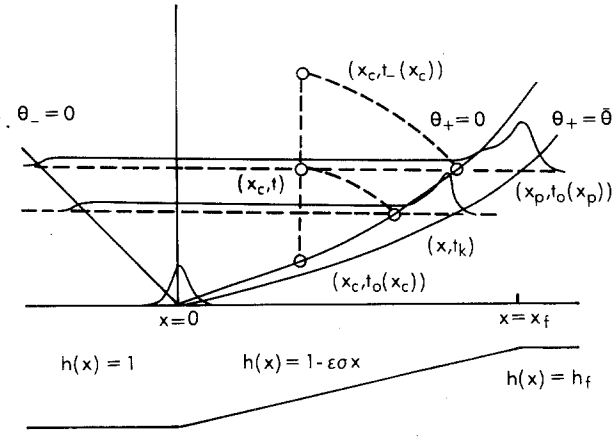

Fig. 4. This figure shows the evolution of a portion of the left-going reflection. The point $(x_p, t_0(x_p))$ lies along $\Theta_+ = 0$ and corresponds to the rear position of the right-going shelf. The line $x = x_c$ corresponds to the station at which the reflected mass flux is to be measured and (x_c, t) is any point on the line between $(x_c, t_0(x_c))$ and $(x_c, t_-(x_c))$. The point (x, t_k) is the intersection of the left-going characteristic through (x_c, t) and $\Theta_+ = 0$.

characteristic $\theta_+ = 0$) and $(x_c, t_-(x_c))$ (which is the left-going characteristic initiated at $(x_p, t_0(x_p))$. Therefore

$$\int_{-\infty}^{\infty} h(x_c)\, u_-(x_c, t)\, dt = \int_{t_0(x_c)}^{t_-(x_c)} h(x_c)\, u_-(x_c, t)\, dt$$

We will convert this integration in t from $t_0(x_c)$ to $t_-(x_c)$ to an integration from $x = x_c$ to x_p along $\theta_+ = 0$. From (2.22a),

$$h(x_c)\, u_-(x_c, t) = h(x)\, u_-(x, t_k)$$

where (x, t_k) is the point of intersection of $\theta_+ = 0$ and the left-going characteristic propagating through (x_c, t).

This implies that

$$t_k + \int_0^x h^{-1/2}(r)\, dr = t + \int_0^{x_c} h^{-1/2}(r)\, dr$$

or

$$t = t_k + \int_0^x h^{-1/2}(r)\, dr - \int_0^{x_c} h^{-1/2}(r)\, dr \tag{2.25}$$

Also at the point (x, t_k), we have that

$$-t_k + \int_0^x h^{-1/2}(r)\, dr = 0 \tag{2.26}$$

This gives us a relationship between t and x. From (2.25) and (2.26) we have

$$t = 2\int_0^x h^{-1/2}(r)\, dr - \int_0^{x_c} h^{-1/2}(r)\, dr$$

or

$$dt = 2h^{-1/2}(x)\, dx \tag{2.27}$$

Therefore the reflected mass flux is (Fig. 4)

$$\int_{-\infty}^{\infty} h(x_c)\, u_-(x_c, t)\, dt = \int_{t_0(x_c)}^{t_-(x_c)} h(x_c)\, u_-(x_c, t)\, dt$$

$$= \int_{t_0(x_c)}^{t_-(x_c)} h(x)\, u_-(x, t_k)\, dt$$

or from (2.19) and (2.27)

$$= \frac{2}{3}\eta_0 \int_{x_c}^{x_p} h^{-3/4}\, dh$$

$$= \tfrac{8}{3}\eta_0 h^{1/4}(x_p) - \tfrac{8}{3}\eta_0 h^{1/4}(x_c)$$

Once the solitary wave has reached a constant depth ($x > x_f$) the mass flux associated with the reflected wave along any x is

$$m_-(x) = \int_{-\infty}^{\infty} h(x)\, u_-(x, t)\, dt = \frac{8}{3}\eta_0 h_f^{1/4} - \frac{8}{3}\eta_0 h^{1/4} \tag{2.28}$$

Adding this result to (2.12) and (2.16), the flux associated with the right-going component, we obtain for the total flux

$$\int_{-\infty}^{\infty} h(x)\, u(x, t)\, dt = \frac{8}{3}\eta_0 h_f^{1/4} \tag{2.29}$$

which is a constant and equal to the flux of the right-going component once the solitary wave has reached the point at which the depth again becomes constant.

In order to calculate the amplitude of the reflected wave n_-, we solve the linear Goursat problem defined as

$$\begin{aligned} n_{-t} + (hu_-)_x &= 0 \\ u_{-t} + n_{-x} &= 0 \\ u_-(\Theta_+ = 0) &= \frac{1}{3}\eta_0 h^{-5/4}(x)\frac{dh}{dx}(x) \\ u_-(\Theta_- = 0) &= 0 \\ n_-(\Theta_- = 0) &= 0 \end{aligned} \tag{2.30}$$

The reason that n_- is not equal to $-h^{1/2}u_-$ [in a manner analogous to $n_+ = \sqrt{h}\,u_+$ for the right-going flow (2.4)] is that the premise by which the latter is derived neglects the smaller term $h_x u_+$. One can not make this assumption for the reflected flow.

In the following section we show the results of solving the Goursat problem numerically and verify that the analysis holds to well within any numerically induced errors.

3. NUMERICAL INTEGRATION OF THE FULL SHALLOW WATER EQUATIONS

In order to verify the results presented in Section 2, we numerically simulated (2.1), (2.2), the full two-directional shallow water equations. This simulation involved the use of a second-order accurate finite difference scheme with a variable spatial mesh.

Table I. Comparison of the Numerical Right-Going Mass Flux and the Analytical Right-Going Mass Flux

Position	Depth	Analytical $= 8\eta_0 h^{1/4}(x)/3$	Numerical	Percent error
$x = 25$	0.976	3.05	2.99	1.97
$x = 101$	0.901	2.99	2.92	2.34
$x = 202$	0.803	2.90	2.84	2.07
$x = 308$	0.693	2.80	2.73	2.50
$x = 372$	0.637	2.74	2.66	2.92
$x = 432$	0.578	2.67	2.58	3.37
$x = 490$	0.521	2.61	2.51	3.83

All the numerical results presented here use $\varepsilon = 1/64$, $\sigma = 1/16$, $\eta_0 = 1.15$, $h_0 = 1$, $h(x) = 1 - \varepsilon\sigma x$, $h_f = 1/2$, $x_f = 512$, $\Delta t = 0.075$, and

$$\Delta x_i = \Delta t\,[h(x_i)^{1/2}][1 + 2\varepsilon\eta_0^2 h^{-2}(x_i)/3]$$

chosen so that $\Delta x_i/\Delta t$ is the velocity of the solitary wave.

Since the analysis depends heavily on the mass flux requirements, we first checked the right-going and total mass flux laws at various stations between $x = 0$ and $x = x_f$ ($h_f = 1/2$). The results of the comparison of the numerical and analytical right-going mass flux are given in Table I.

Table II. Mass Flux and Change in Mass Flux at Various Positions in the x, Θ_- Plane[a]

x:	−9.9	24.8	101.3	202.1	308.4	371.4	432.0	487.6	547.5
$\Theta_- h(x)$:	1.00	0.98	0.90	0.80	0.70	0.64	0.58	0.52	0.5
1400	2.55	2.55	2.53	2.52	2.50	2.49	2.49	2.48	2.48
	0.00	0.00	0.01	0.01	0.00	0.00	0.00	0.00	
1300	2.55	2.55	2.53	2.51	2.50	2.49	2.49	2.48	
	0.00	0.00	0.00	0.00	0.00	0.01	0.00	0.01	
1200	2.55	2.55	2.53	2.51	2.50	2.50	2.49	2.49	
	0.04	0.04	0.04	0.05	0.05	0.05	0.05		
1100	2.60	2.59	2.58	2.56	2.55	2.55	2.54		
	0.04	0.04	0.04	0.05	0.05	0.04			
1000	2.64	2.63	2.62	2.61	2.60	2.59			
	0.04	0.05	0.05	0.04	0.04	0.05			
900	2.68	2.68	2.67	2.65	2.64	2.64			
	0.04	0.04	0.04	0.05	0.05				
800	2.72	2.72	2.71	2.70	2.69				
	0.04	0.04	0.04	0.04	0.04				
700	2.76	2.76	2.75	2.74	2.73				
	0.04	0.04	0.04						
600	2.80	2.80	2.79						
	0.04	0.03							
500	2.84	2.83							
	0.04	0.04							
400	2.88	2.87							

[a] Within each entry of the table the top number is the total mass flux measured along a constant x from $t = -\infty$ up to that left-going characteristic $\Theta_- = t + \int_0^x h^{-1/2}(r)\,dr$. The bottom number is the mass flux measured between two consecutive left-going characteristics listed in the table.

Table III. Mass Flux and Change in Mass Flux Measured Along a Constant x ($x = 371.5$) at Various Times[a]

Time	Mass flux	Change in mass flux
	Solitary wave	
423.0	0.04	-0.04
424.5	1.78	-1.74
426.0	1.98	-0.20
427.5	2.09	-0.11
	Right-going shelf	
429.0	2.22	-0.13
430.5	2.37	-0.15
432.0	2.52	-0.15
433.5	2.63	-0.05
534.0	2.68	-0.05
	Oscillitory tail	
436.5	2.67	0.39×10^{-2}
444.0	2.66	-0.18×10^{-2}
451.5	2.65	0.85×10^{-3}
459.0	2.65	0.11×10^{-2}
	Left-going reflection	
465	2.65	0.91×10^{-3}
570	2.60	0.69×10^{-3}
666	2.56	0.70×10^{-3}
787.5	2.50	0.73×10^{-3}
	No further reflection	
796.5	2.49	0.26×10^{-3}
851.0	2.49	0.20×10^{-4}
948	2.49	0.40×10^{-5}

[a] The first column gives the time units (note the difference in the time scales between the various sections), the second column represents the total mass flux measured at $x = 371.5$ up to the given time, and column 3 gives the mass flux measured only over the previous 1.5 time units.

In Table II, we display the numerical results for the mass flux

$$m(x, \Theta_-) = \int_{-\infty}^{t} hu\, dt, \qquad t_- = \Theta_- - \int_0^x \frac{dr}{\sqrt{h}}$$

and the increment

$$\Delta m(x, \Theta_-) = m(x, \Theta_- - \Delta\Theta_-) - m(x, \Theta_-)$$

as function of Θ_-, $0 < \Theta_- < 1400$ for several stations x. The negative characteristic $\Theta_- = 1200$ is the one which passes through the intersection of $\Theta_+ = 0$ and $x = 512$, $h(512) = \frac{1}{2}$. This would be the last characteristic on which information is carried back if the transition along $\Theta_+ = 0$ between right- and left-going flow components was sharp. In actual fact, the transition is described by an Airy function[9] and occurs over a width of $\sigma^{-1/3}$ times the width of the solitary wave. Indeed we shall see in Table III this is the width of the transition along $\Theta_- = 1200$. Note that the data are consistent with our picture that the reflected wave generated along $\Theta_+ = 0$ between $\Theta_- - \Delta\Theta_-$ and Θ_- is carried back through this tube. In particular, both $m(x, \Theta_-)$ and $\Delta m(x, \Theta_-)$ are independent of x to within the order of approximation of Eq. (2.3) (approximately 3%). Moreover $m(x, \Theta_-)$, $0 < \Theta_- < 1200$ is precisely the total right-going flux at the station at which the curve $\Theta_- = t + \int_0^x dx/\sqrt{h}$ meets $\Theta_+ = 0$ and would be the total mass flux if the depth were to become constant after this point. We emphasize that the reflection is generated all along $\Theta_+ = 0$. In order to make sure that the discontinuities in $h(x)$ at $x = 0$ and $x = 512$ play no significant role, we repeated the calculation with a cubic-shaped bottom.

Table IV. Comparison at Various Depths of the Analytical and Numerical Times at Which No Further Reflection is Measured[a]

x	$h(x)$	Analytic time	Numerical time
24.8	0.98	1175	1180
101.3	0.90	1096	1101
202.1	0.80	987	991
308.4	0.70	864	867
371.4	0.64	787	791
432.0	0.58	709	714
487.6	0.52	634	633

[a] The analytical time is calculated from $t = 1200 - \int_0^x h^{-1/2}(r)\, dr$, while the numerical time is given as the time at which the change in the mass flux decreases by a factor of 2.

Table III displays the incremental mass flux $\Delta m(x, t) = m(x, t) - m(x, t - 1.5)$ for $x = 371.5$. Note the solitary wave, the right-going shelf, the oscillatory tail, the long reflection, and the sharp drop at the "last" negative characteristic $\Theta_- = 1200$. Table IV is a comparison at several stations x of the times $t = 1200 - \int_0^x (dx/\sqrt{h})$ and the times in the numerical experiment at which the increment in the reflected mass flux decreased by a factor of 2.

The total mass flux, which is the right-going flux at $x = x_f$ and equal to 2.58 for the parameters given above, was measured at various stations and found to be a constant to within 4.5%. The error in the mass flux was expected since (2.3) is not an exact conservation law of equations (2.1) and (2.2). But, upon integrating (2.2) with respect to t we find the exact conservation law

$$\frac{\partial}{\partial x} \int_{-\infty}^{\infty} \left(n + \frac{\varepsilon u^2}{2} \right) dt = 0$$

This quantity was measured at various stations and found to be a constant to within less than 1%.

We also checked various components of the analytical solution against the numerical results. First, we compared the maximum horizontal velocity of the analytical solitary wave $[\max(u_s(x, t)] = 4\eta_0 h^{-3/2}(x)/3$ against the maximum horizontal velocity of the numerical solitary wave. The results of this comparison can be found in Table V. A graphical representation of the comparison between the numerical and analytical solitary waves at $t = 500$ can be found in Fig. 5. We also checked the analytical predictions of the

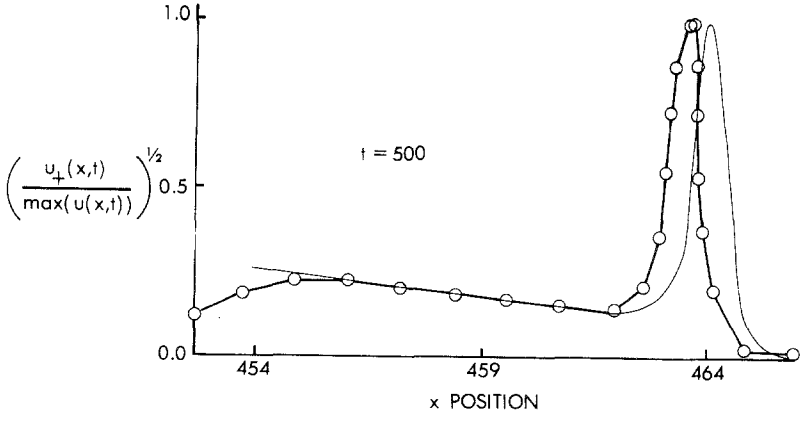

Fig. 5. This figure shows a comparison between the numerical right going flow (–◦–) and the analytical right-going flow (–) versus the spatial coordinate x at time $t = 500$. Both curves were scaled by taking the square root of the normalized value.

Table V. Comparison of the Maximum Analytical Horizontal Velocity and the Maximum Numerical Horizontal Velocity at Various Positions

Numerical position	Depth	Analytical = $4\eta_0^2 h^{-3/2}(x)/3$	Numerical	Percent error
10.4	0.99	1.79	1.76	1.5
99.3	0.90	2.05	1.96	4.4
211.9	0.79	2.50	2.37	4.9
317.8	0.69	3.08	2.93	5.0
417.6	0.59	3.86	3.69	4.4
509.7	0.50	4.95	4.76	4.0

horizontal velocity for the right shelf against the numerical experiment. The results of this comparison can also be seen in Fig. 5. Except for a slight phase shift (less than 5%), the reader can see that the analytical predictions and the numerical results for the right-going flow are very close.

The numerical evidence supports our theoretical picture which asserts that the right-going flow component is described by the perturbed Korteweg–deVries equation (2.8) and the left-going flow component is found by solving the Goursat problem (2.30). While Table II showed clearly that the incremental mass flux carried through the tubes $(\Theta_- - \Delta\Theta_-, \Theta_-)$ is constant in x, we would like to verify (2.22) along each negative characteristic individually. This is not possible to do using the results of the first numerical scheme because even though the mass flux data is accurate, the pointwise data are not sufficiently good. Accordingly, we solved the Goursat problem defined by (2.30) numerically and found

1. $n_- + h^{1/2}u_-$ is independent of time along a constant x;
2. hu_- and n_- [(2.22a), (2.22b), respectively] are constants along left going characteristics;
3. the reflected mass flux is given by (2.28).

Table VI. A Comparison of $(\partial/\partial t)(n_- + h^{1/2}u_-)$ and $(\epsilon\sigma)^3$ for Various $\epsilon\sigma$

x	$h(x)$	$\varepsilon\sigma$	$(\varepsilon\sigma)^3$	$\frac{\partial}{\partial t}(n_- + h^{1/2}u_-)$
25.6	0.95	1/512	7.5×10^{-9}	6.4×10^{-9}
25.6	0.90	2/512	6.0×10^{-8}	5.1×10^{-8}
25.6	0.80	4/512	4.8×10^{-7}	4.0×10^{-7}
25.6	0.70	6/512	1.6×10^{-6}	1.8×10^{-6}
25.6	0.65	7/512	2.6×10^{-6}	6.2×10^{-6}

Table VII. A Comparison of the Changes in hu_- and n_- with $(\epsilon\sigma)^3$ for Various Slopes $\epsilon\sigma$ Along $\Theta_- = 101$

$\varepsilon\sigma$	$\varepsilon^3\sigma^3$	$\left(\frac{\partial}{\partial t}+h^{1/2}\frac{\partial}{\partial x}\right)(hu_-)$	$\left(\frac{\partial}{\partial t}+h^{1/2}\frac{\partial}{\partial x}\right)n_-$
1/128	4.8×10^{-7}	2.1×10^{-7}	2.3×10^{-7}
1/256	6.0×10^{-8}	2.4×10^{-8}	2.4×10^{-8}
1/512	7.5×10^{-9}	4.6×10^{-9}	4.3×10^{-9}
1/1024	9.3×10^{-10}	8.0×10^{-10}	7.6×10^{-10}

We first checked the mass flux, $\int_{-\infty}^{\infty} hu_- \, dt$, given by the numerical experiment against (2.28) and found close agreement. The relative error was much less than 1% for all cases.

We next checked the constancy of $n_- + h^{1/2}u_-$ along a constant x. Because n_- and $h^{1/2}u_-$ are of the order of $\varepsilon\sigma$ and their individual time derivatives are of the order of $\varepsilon^2\sigma^2$, we must show that the time derivative of the sum is small with respect to $\varepsilon^2\sigma^2$. The numerical experiments showed that the average of the gradient of $n_- + h^{1/2}u_-$ was of the order of $\varepsilon^3\sigma^3$. These results are shown in Table VI.

We also checked hu_- and n_- along negative characteristics [(2.22a), (2.22b), respectively] and found that the changes in hu_- and n_- along negative characteristics were of the order of $\varepsilon^3\sigma^3$. Table VII contains the results from various cases checked along a typical Θ_- characteristic.

REFERENCES

1. J. Boussinesq, Théorie des ondes des remous qui se propagert le long d'un rectangulaire horizontal, en communiquant au liquide contenu dans ce canal des sensiblenert pareilles de la surface au fond, *J. Math. Pures Appl.* **17**:55–108 (1872).
2. R. Grimshaw, The Solitary Wave in Water of Variable Depth, *J. Fluid Mech.* **42**(3):639–656 (1970).
3. R. Grimshaw, The Solitary Wave in Water of Variable Depth, Part 2, *J. Fluid Mech.* **46**(3):611–622 (1971).
4. R. S. Johnson, Asymptotic Solution of the Korteweg–deVries with Slowly Varying Coefficients, *J. Fluid Mech.* **60**(4):813–824 (1973).
5. R. S. Johnson, On the Development of a Solitary Wave Moving Over an Uneven Bottom. *Proc. Cambridge Philos. Soc.* **73**:183 (1973).
6. T. Kakutani, Effects of an Uneven Bottom on Gravity Waves, *J. Phys. Soc. Jpn* **30**:272 (1971).
7. V. I. Karpman and E. M. Maslov, A Perturbation Theory for the Korteweg–deVries Equation, *Phys. Lett.* **60A**:307–308 (1977).
8. D. J. Kaup and A. C. Newell, Solitons as Particles and Oscillators and in Slowly Varying Media: A Singular Perturbation Theory, *Proc. R. Soc. London* **A361**:413–446 (1978).

9. C. J. Knickerbocker and A. C. Newell, Shelves and the Korteweg–deVries Equation, *J. Fluid Mech.* **98**(4):803–818 (1980).
10. C. J. Knickerbocker, Ph.D. dissertation, Clarkson University (1984).
11. C. J. Knickerbocker and A. C. Newell, Reflections from Solitary Waves in Channels of Decreasing Depth, *J. Fluid Mech.*, to appear (1985).
12. D. J. Korteweg and G. deVries, On the Change of Form of Long Waves Advances in a Rectangular Canal, and on the New Type of Long Stationary Waves, *Phil. Mag.* **5**(39):422 (1895).
13. S. Leibovich and J. D. Randall, Amplification and Decay of Long Nonlinear Waves, *J. Fluid Mech.* **58**(3):481–493 (1973).
14. J. W. Miles, On the Korteweg–deVries Equation for a Gradually Varying Channel, *J. Fluid Mech.* **91**:181–190 (1979).
15. A. C. Newell, Soliton Perturbation and Nonlinear Focussing, Symposium on Nonlinear Structure and Dynamics in Condensed Matter, *Solid State Phys.* **8**:52–68 (1978).
16. D. H. Peregrine, Long Waves on a Beach, *J. Fluid Mech.* **27**:815 (1967).